Electro-catalytic degradation of sulfisoxazole by using graphene anode

Yanyan Wang[1], Shuan Liu[2], Ruiping Li[1], Yingping Huang[1,*], Chuncheng Chen[1,*]

1. Collaborative Innovation Center for Geo-Hazards and Eco-Environment in Three Gorges Area, Yichang 443002, China
2. Key Laboratory of Marine New Materials and Application Technology, Ningbo Institute of Materials Technology and Engineering, Chinese Academy of Sciences, Ningbo 315201, China

ARTICLE INFO

ABSTRACT

Graphite and graphene electrodes were prepared by using pure graphite as precursor. The electrode materials were characterized by a scanning electron microscope (SEM), X-ray diffraction (XRD) and cyclic voltammetry (CV) measurements. The electro-catalytic activity for degradation of sulfisoxazole (SIZ) was investigated by using prepared graphene or graphite anode. The results showed that the degradation of SIZ was much more rapid on the graphene than that on the graphite electrode. Moreover, the graphene electrode exhibited good stability and recyclability. The analysis on the intermediate products and the measurement of active species during the SIZ degradation demonstrated that indirect oxidation is the dominant mechanism, involving the electro-catalytic generation of $\cdot OH$ and O_2^- as the main active oxygen species. This study implies that graphene is a promising potential electrode material for long-term application to electro-catalytic degradation of organic pollutants.

© 2015 The Research Center for Eco-Environmental Sciences, Chinese Academy of Sciences. Published by Elsevier B.V.

Introduction

Because of its unique structure and properties, graphene, a single layer of graphite, has been receiving increasing attention in the catalytic, optical, electrical, and magnetic fields (Geim, 2009; Wang et al., 2009; Henrik and Peter, 2010; Guo et al., 2009). This makes graphene sheets a highly promising electro-catalyst or catalyst support (Bong et al., 2010). As electrode material, the performance of graphene is usually superior to the conventional carbon materials like graphite and active carbon because of its enriched surface sites, high specific surface area, high electrical conductivity, and chemical stability (Yan et al., 2010; Liu et al., 2013a, 2013b). Although the electro-catalytic activity of graphene-based electrodes has been extensively studied for processes such as oxygen reduction and H_2 production (Benson et al., 2014),

little attention has been given to its application in the electro-catalytic degradation of organic pollutants.

In addition, the residues of sulfa antibiotics have raised serious environmental problems because of their extensive use in a variety of human and veterinary applications and resistance to biodegradation. In our previous study, it was demonstrated that residues of antibiotics like tetracycline can be degraded by electro-catalytic methods (Liu et al., 2013a), and a graphite composite electrode exhibited excellent potential for removing persistent organic pollutants (POPs) in wastewater (Liu et al., 2013b). In the present work, our aim was to investigate the electro-catalytic reactivity for oxidative degradation of sulfa antibiotic pollutants using sulfisoxazole (SIZ) as a model. The mechanistic study suggested that the hydroxyl radical is responsible for the degradation of SIZ on the graphene electrode. The present

* Corresponding authors. E-mail: chem_ctgu@126.com (Yingping Huang), ccchen@iccas.ac.cn (Chuncheng Chen).

work highlights the promising potential of graphene in the application of environmental remediation.

1. Experimental

1.1. Reagents

SIZ solution (30 mg/L) and horseradish peroxidase (POD) solution (0.10%) were prepared and stored in the dark at low temperature (<4°C). A 0.30% H_2O_2 solution was calibrated using $KMnO_4$. N,N-diethyl-p-phenylenediamine (DPD) aqueous solution (1.0%) was prepared just before its use. Other chemicals were analytical grade. Distilled water was used throughout the experiments.

1.2. Instrumentation

The graphene was prepared by a two-step method: graphite oxide (GO) was obtained first and then was reduced to graphene by using hydrazine hydrate (Raj and John, 2013). Then 1.2 g graphite or graphene, 200 μL emulsifier OP-10 (OP) emulsifier, 0.4 mL ethanol and 0.7 mL polytetrafluoroethylene emulsion were added sequentially to a 50 mL beaker. The subsequent ultrasonic treatment dispersed the mixture into a condensed paste. The paste was rolled into 2 mm membranes and attached to a stainless steel net. Under a pressure of 20 MPa, it was compressed into electrodes, followed by washing with ethanol and distilled water to neutrality and then dried in an infrared box for 2 hr at 80°C. Electrochemical analysis of electrodes was performed using a three-electrode system with an AUTOLAB analyzer to measure the I–V loop curve, at a scanning speed of 50 mV/s.

SIZ was chosen as a target contaminant and samples were collected at specific time intervals for high-performance liquid chromatography (Agilent 1220, American) measurement after filtration. The chromatograph was equipped with a C18 reverse phase column (5 μm, 4.6 mm I.D. × 250 mm, Kromasil) as stationary phase. The mobile phase was 0.1% HCOOH and CH_3CN ($V:V$ = 65:35) with a flow rate of 1 mL/min, column temperature at 30°C, 20 μL of sample volume, and at 275 nm wavelength. The solvent was removed with a rotary evaporator and the structure and morphology of the samples were analyzed by a Fourier transform infrared spectrometer (Nicolet, American).

The H_2O_2 concentration measurement was conducted with a UV–Vis spectrophotometer (Lambda-25, PerkinElmer, American) at 510 nm using a 10 mL colorimetric cuvette with plug, 10 min after addition of 150 μL 1.0% DPD, 1 mL pH 6.8 KH_2PO_4 buffer solution, 20 μL 0.1% POD into the 1 mL sample. The total volume was made up to 5 mL with addition of distilled water. Determination of O_2^- was performed using 2.5×10^{-5} mol/L Nitrotetrazolium Blue chloride solution as trapping reagent. The sample was collected at specific time intervals for absorbance measurement at 259 nm using the UV–Vis spectrophotometer. Similar to O_2^-, the determination of ·OH used 5×10^{-4} mol/L terephthalic acid as trapping reagent for the relative fluorescence intensity measurement (Ex = 315 nm, Em = 425 nm, and slit widths 5 nm and 10 nm, respectively).

Liquid phase mass spectrometry equipped with a C18 reversed phase column as stationary phase (Poroshell 120 SB-C18, 150 × 4.6 mm, 2.7 μm) used 0.1% formic acid and acetonitrile ($V:V$ = 80:20) as mobile phase at a flow rate of 4 mL/min. The other operational parameters were the same as mentioned above.

2. Results and discussion

2.1. Characterization of graphite and graphene powers

Scanning electron microscope (SEM) analysis of graphite and graphene is shown in Fig. 1. The graphite flake had a smooth surface with a size of several tens of micrometers and thickness of less than 5 μm. In contrast, graphene exhibited obvious fold morphology, and the regular layered structure of graphite disappeared. Such a structure would increase its plasticity, and should be the origin of the unique thermal, electrical, and mechanical properties of graphene (Yuan et al., 2013).

X-ray diffraction (XRD) patterns of graphite and graphene are shown in Fig. 2. For graphite, a sharp and strong peak at around 26.3° accorded with its standard XRD data (PDF41-1487). Calculated by prague formula, the graphite (002) crystal plane spacing was about 0.34 nm. Due to partial oxidation of the graphite surface (Han and Wang et al., 2003), there was a small diffraction peak of GO at around 54.5°. Compared with graphite, the XRD peak of graphene showed a negative shift to around 24.8°, suggesting that the graphene layer spacing was slightly greater than that of graphite (0.34 nm). In addition, the diffraction peak of graphene became wider and weaker.
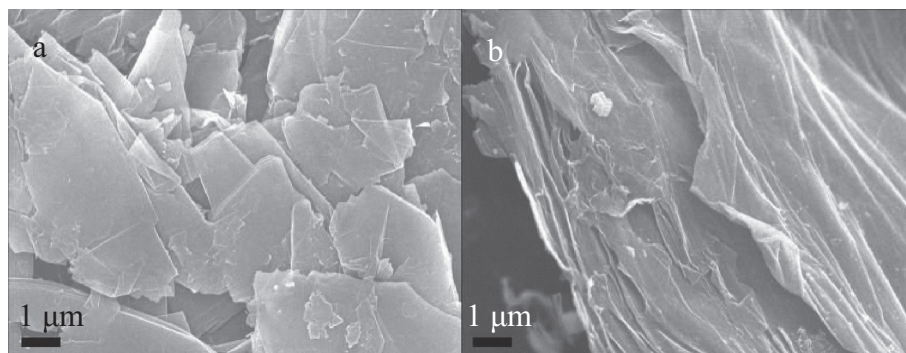

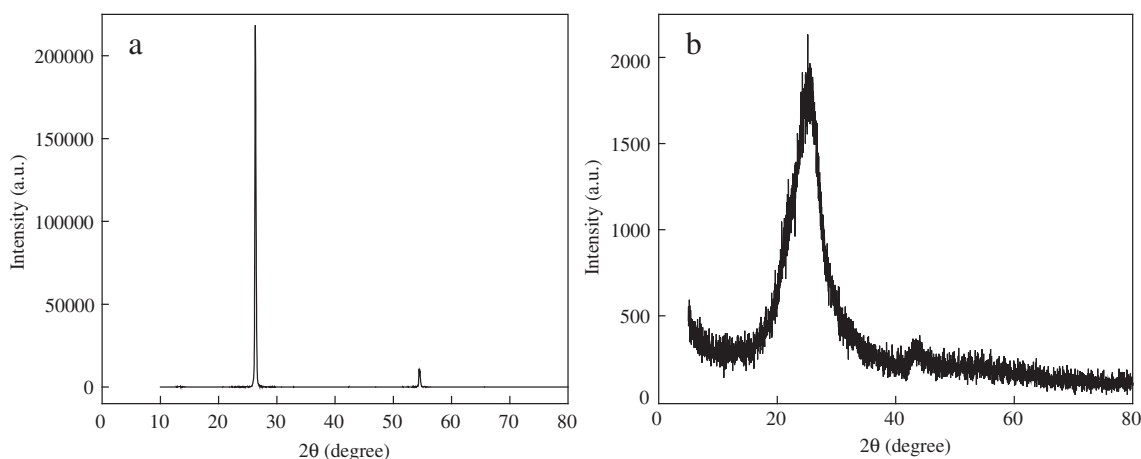**Fig. 1 – Scanning electron microscope (SEM) images of graphite (a) and graphene (b) powder.**

Fig. 2 – X-ray diffraction (XRD) patterns of graphite (a) and graphene (b) powders.

2.2. Electrochemical analysis of graphite and graphene electrodes

The results of cyclic voltammetry (CV) in Fig. 3 show a pair of quasi-reversible cathodic and anodic current peaks for both graphite and graphene electrodes, indicating that both of them had some capacitance and could store electrical energy. The capacitance of graphite was slightly greater than that of graphene ($H > h$). It was reported previously that greater capacitance for an electrode material would lead to poorer cycle performance (Jin et al., 2013). From this aspect, the graphene electrode is better than graphite.

2.3. Degradation of SIZ by electro-catalysis on graphite and graphene electrodes

Electro-catalytic degradation of SIZ by electrodes made from different materials is shown in Fig. 4a. Only 19% of SIZ was removed with the stainless steel net as anode after electrolysis of 180 min. The SIZ removal efficiency increased to 76% using the graphite electrode. Interestingly, SIZ was almost completely removed using the graphene electrode, indicating that the graphene electrode has superior activity for the degradation reaction compared to graphite. The degradation products of SIZ using the graphene electrode were identified by HPLC (Fig. 4b). The growth of peaks from the different degradation products was accompanied by rapid SIZ degradation (peak at 5.78 min). The predominant degradation products showed peaks around 0.80 min and 1.91 min. To test the stability of the graphene electrode, a cycling experiment was conducted and presented in Fig. 4c, demonstrating that no decrease of performance was observed after 5 cycles, indicative of the excellent stability of the graphene electrode. FT-IR was used to characterize SIZ electro-catalytic degradation by the graphene electrode. As illustrated in Fig. 4d, the spectrum of SIZ exhibited several strong peaks at 1990 cm^{-1} (molecular skeleton vibration), 1650–1500 cm^{-1} (bending vibration of N = H), 1360–1000 cm^{-1} (stretching vibration of C–N in the aniline group), 940 cm^{-1} (breathing vibration of oxazole ring), and 1200 cm^{-1}, 620 cm^{-1} and 500 cm^{-1} (stretching vibration of sulfonic acid group (–SO$_2$–)) (Shinozuka et al., 2001; Shylesh et al., 2007). During

its electro-catalytic degradation, the intensity of these characteristic peaks gradually decreased and nearly disappeared after 180 min, indicating that the molecular structure of SIZ was destroyed gradually.

HPLC-MS was further performed to track the formation of other intermediates during the SIZ electro-catalytic degradation. According to the HPLC-MS analysis (Fig. 5), we could speculate that ammonia, esters, carboxylic acid and some other products were the final degradation products. It is also notable that formation of all the detected intermediates can be well explained by the attack of $^{.}OH$ or O_2^- radicals on the substrate or on the intermediates, as discussed below.

2.4. Active species analysis during SIZ degradation

The active oxygen species such as H_2O_2, O_2^- and $^{.}OH$, which are known to be the dominant active species for the degradation of organic pollutants in many oxidative systems, were further examined during SIZ degradation. As shown in Fig. 6, for both the H_2O_2 and O_2^-, their concentrations increased gradually at the initial stage, and reached the maximum at 90 min in the graphene system (Fig. 6a and b). After that their concentration
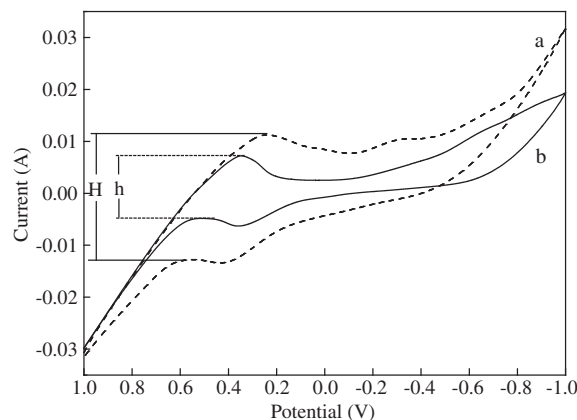

Fig. 3 – Cyclic voltammetry (CV) of graphite (line a) and graphene (line b) electrodes in Na$_2$SO$_4$ solution at 25°C.
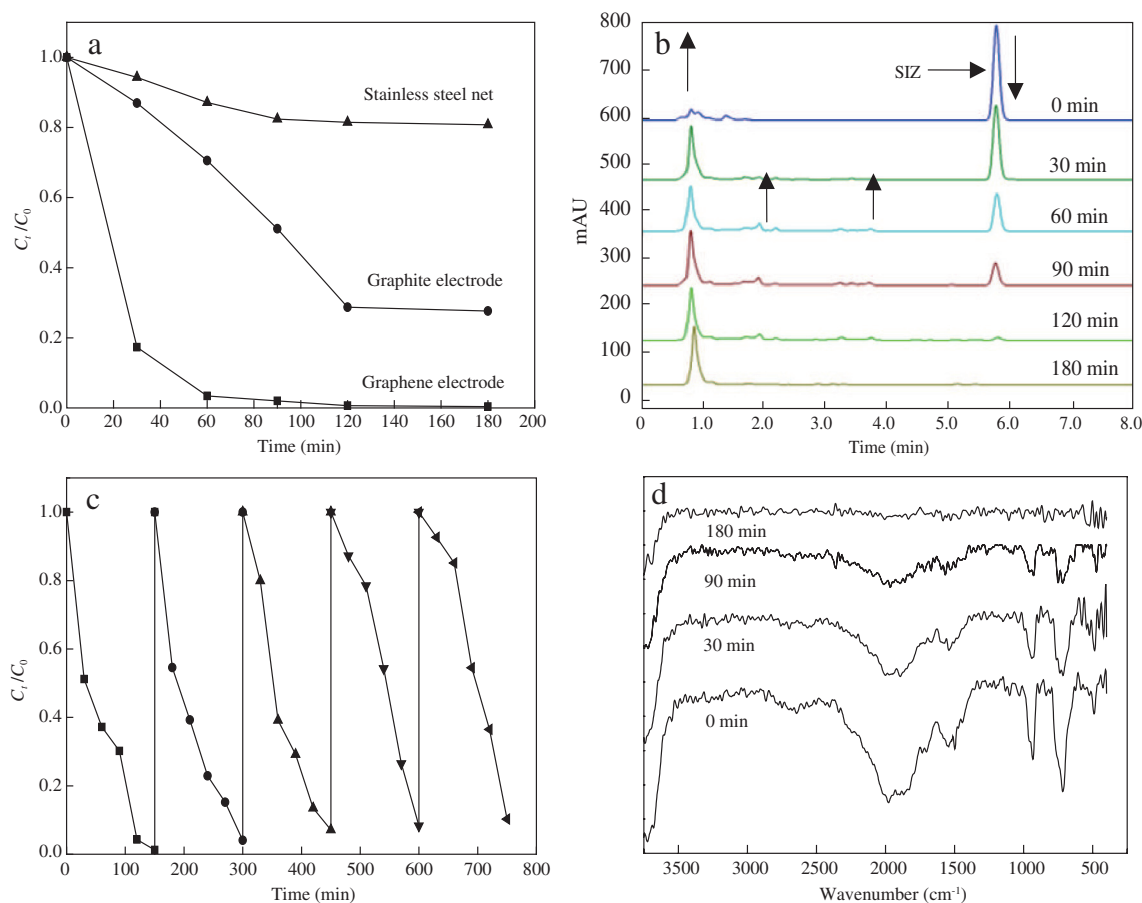
Fig. 4 – Kinetic curves of sulfisoxazole (SIZ) degradation (a), high performance liquid chromatography (HPLC) of SIZ on graphene (b), stability test of graphene electrode (c), Fourier transform infrared spectrometer (FT-IR) spectrum of SIZ at different times (d) during the electro-catalytic degradation. Potential = 1.5 V *vs.* Saturated calomel electrode (SCE), Na$_2$SO$_4$ = 10 g/L, SIZ concentration = 30 mg/L.

decreased with the extension of reaction time. The presence of a maximum for the concentration of H$_2$O$_2$ and O$_2^-$ is indicative of their formation and depletion on the graphene electrode. However, on the graphite electrode, the concentration of H$_2$O$_2$ was gradually increased, and no decrease was observed within the tested electrolytic time, while the amount of O$_2^-$ was not changed much, which may result from the similar rates for the formation and consumption of O$_2^-$ during the electrolysis. The formation of ·OH was estimated by using terephthalic acid as trapping reagent, and the fluorescence measurement for the formed hydroxylated terephthalic acid would reflect the relative amount of ·OH in the reaction systems. As shown in Fig. 6c and d, the fluorescence intensity of the hydroxylated terephthalic acid was much stronger in the graphene system, and the maximum intensity was about 2.5 times that in the graphite system. The different amounts and change trends of O$_2^-$, H$_2$O$_2$ and ·OH indicate that the superior activity of the graphene electrode can be attributed to its different electro-catalytic behavior in the activation of H$_2$O and the H$_2$O$_2$ intermediate to active species. In electro-catalytic systems, anodic oxidation of H$_2$O would lead to the formation of OH· (Eq. (1)), which has strong oxidative ability and can directly degrade organic pollutants (Zhang et al., 2008; Cristina et al., 2006). The higher concentration of ·OH observed is consistent with the higher activity of the

graphene electrode, suggesting that ·OH is responsible for the degradation of SIZ on the graphene, and that the graphene electrode has a superior ability to activate H$_2$O to ·OH. Besides being a direct active species for SIZ degradation, the formed ·OH can couple to H$_2$O$_2$ (Eq. (2)), which is further oxidized to O$_2^-$ (HO$_2$) on the anode (Eq. (4)). The different change trends for O$_2^-$ and H$_2$O$_2$ on the graphite and graphene electrodes indicate that these two electrodes have different behaviors for the formation and decomposition of O$_2^-$ and H$_2$O$_2$. The presence of a maximum for the concentration of H$_2$O$_2$ on the graphene electrode and the absence of a maximum H$_2$O$_2$ concentration on graphite (Fig. 6a and b) suggest that the oxidation of H$_2$O$_2$ to O$_2^-$ on the graphene electrode tends to be easier than that on graphite.

$$H_2O - e^- \rightarrow {}^U OH + H^+ \tag{1}$$

$$2\,{}^{\cdot}OH \rightarrow H_2O_2 \tag{2}$$

$$H_2O_2 - e^- \rightarrow HO_2^{\cdot} + H^+ \tag{3}$$

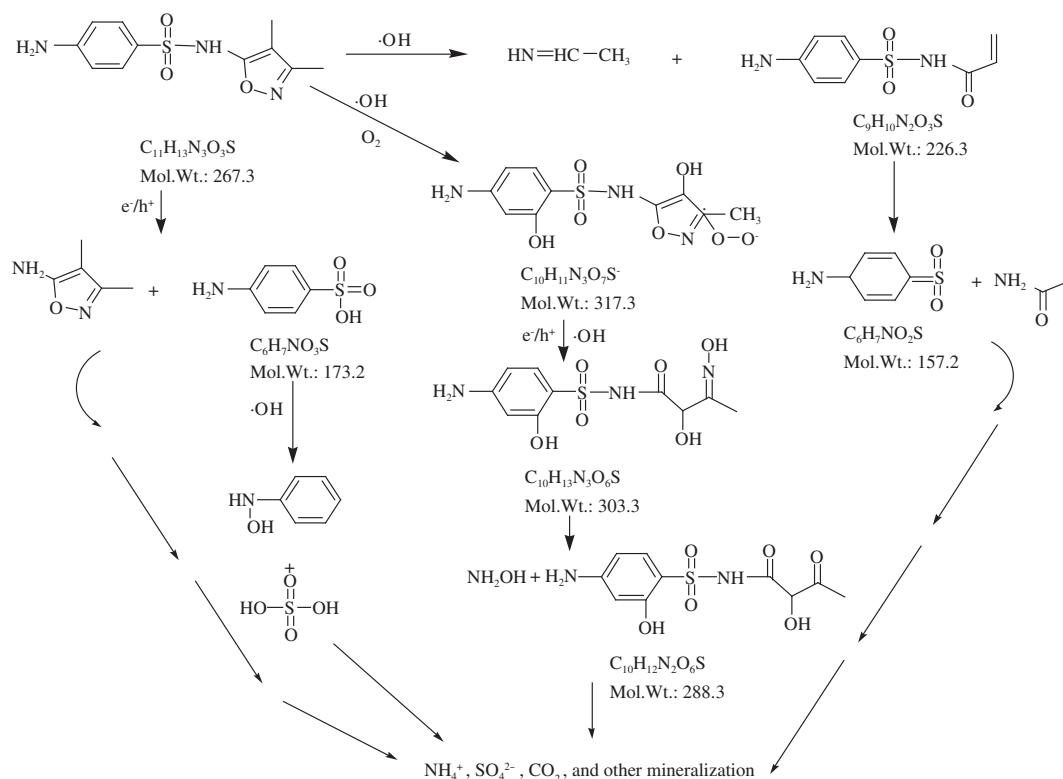$${}^{\cdot}OH(HO_2^{\cdot}) + SIZ \rightarrow Degradation\ products \tag{4}$$

Fig. 5 – Possible degradation pathway of SIZ.

To shed more light on the role of the active oxygen species in the SIZ degradation, various scavengers were added to capture the active species, and their effects on the degradation rate were examined in Fig. 7. When isopropanol (1 mmol/L), benzoquinone (1 mmol/L) and ethylene diamine tetraacetic acid (1 mmol/L) were added to scavenge $\cdot OH$, O_2^- and h^+ respectively, the degradation of SIZ was markedly suppressed, indicating that $\cdot OH$, O_2^-, and h^+ are all involved in the degradation of SIZ. These results are consistent with those on the active species measurement in Fig. 4, and imply that the superior activity of the graphene electrode for the degradation of organic pollutants should stem from its unique catalytic ability to activate water and the H_2O_2 intermediate to generate active oxygen species $\cdot OH$ and HO_2 (Eq. (4)). Since the O_2^- radical has only moderate oxidative ability, relative to the $\cdot OH$ radical, it should be difficult for O_2^- to directly initiate the degradation reaction. More reasonably, O_2^- reacts with the $\cdot OH$ derived radical intermediates, which leads to the fragmentation of pollutant molecules, rather that only hydroxylation, as indicated by the product analysis in Fig. 5. The superior activity of graphene electrodes can be attributed to its special surface properties. It is known that the graphene possesses plenty of defects and functional groups such as epoxide groups, carbonyl (C = O), hydroxyl (–OH) and phenol. These defects and functional groups should be responsible for its higher activity for H_2O activation. These groups are usually hydrophilic and easily hydrated in the water solution. As a result, the charge transfer between the electrode and the adsorbed water is facilitated through these groups. Accordingly,

more reactive species are generated, especially $\cdot OH$, and more rapid degradation of SIZ thus is realized.

We also note that, generally, the electro-catalytic oxidation of organic pollutants can be attributed to direct oxidation and indirect oxidation. The former process involves the direct electron transfer between electrodes to the organic pollutants, while indirect oxidation is mediated by the electrode reaction to produce strongly oxidizing intermediates, which can further degrade the target pollutants (Bunce et al., 1997; Gulppi et al., 2014; Qu et al., 2013; Panizza and Cerisola, 2009). Evidently, the indirect oxidation pathway should be dominant for the electro-catalytic degradation reaction of SIZ on graphene.

3. Conclusions

Using graphene as anode, the electrocatalytic degradation of SIZ was investigated and compared with that on a graphite electrode. The graphene electrode exhibited much higher electro-catalytic activity than the graphite one. Further, the graphene electrode had good recycling performance. The electro-catalytic activity of the graphene anode was proposed to stem from its unique catalytic ability to activate water and the H_2O_2 intermediate to generate the active oxygen species $\cdot OH$ and O_2^-. The present study demonstrates that the graphene electrode can be an excellent electro-catalytic anode for the oxidative degradation of organic pollutants.
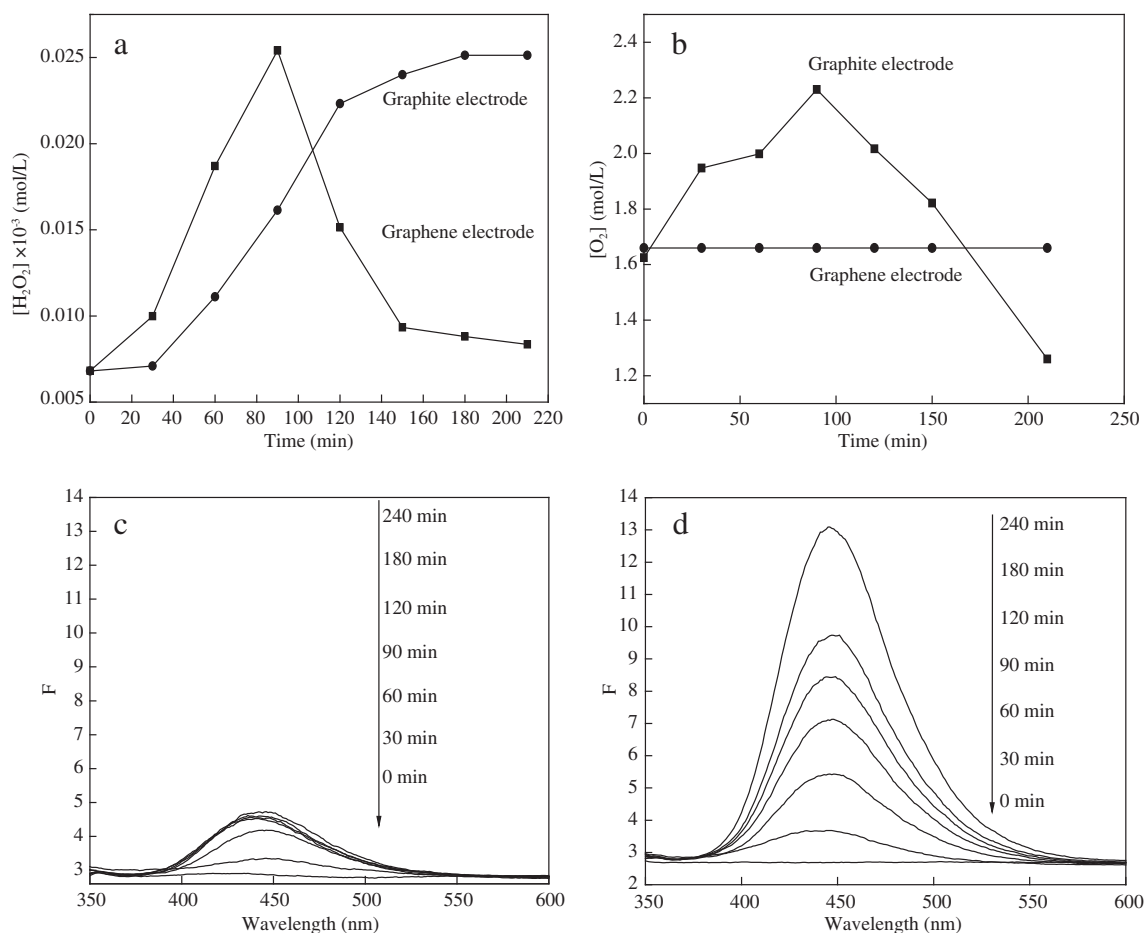
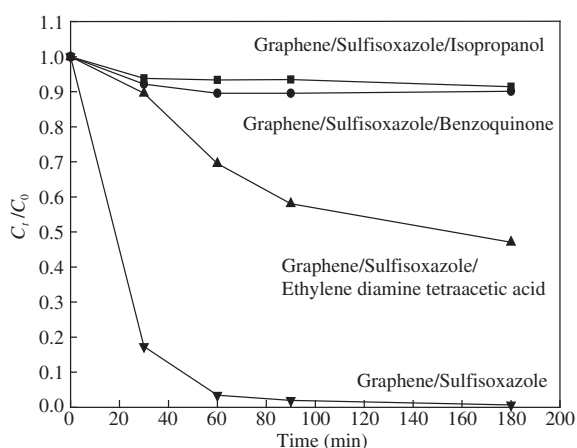**Fig. 6 – Variation of H⁻ (b), ·OH in graphite system (c) and ·OH in graphene system (d) during SIZ degradation.**

Fig. 7 – The degradation of SIZ with addition of the corresponding radical scavengers.

Acknowledgments

REFERENCES

Benson, J., Xu, Q., Wang, P., Shen, Y.T., Sun, L.T., 2014. Tuning the catalytic activity of graphene nanosheets for oxygen reduction reaction via size and thickness reduction. ACS Appl. Mater. Interfaces 6 (22), 19726–19736.

Bong, S., Kim, Y.R., Kim, I., Woo, S., Uhm, S., Lee, J., et al., 2010. Graphene supported electrocatalysts for methanol oxidation. Electrochem. Commun. 12, 129–131.

Bunce, N., Merica, S., Lipkowski, J., 1997. Prospects for the use of electrochemical methods for the destruction of aromatic organochlorine wastes. Chemosphere 35 (11), 2719–2726.

Cristina, F., Salah, A., Conchita, A., Brillas, E., Vargas-Zavala, A.V.V., Abdelhedi, R., 2006. Electro-Fenton and photoelectro-Fenton degradation of indigo carmine in acidic aqueous medium. Appl. Catal., B. 67, 93–104.

Geim, A.K., 2009. Graphene: status and prospects. Sci. 324 (5934), 1530–1534.

Gulppi, M., Recio, F., Tasca, F., Ochoa, G., Silva, J., Pavez, J., et al., 2014. Optimizing the reactivity of surface confined cobalt N₄-macrocyclics for the electrocatalytic oxidation of L-cysteine by tuning the Co(II)/(I)formal potential of the catalyst. Electrochim. Acta 126, 37–41.

Guo, P., Song, H.H., Chen, X.H., 2009. Electrochemical performance of graphene nanosheets as anode material for lithium-ion batteries. Electrochim. Acta 11 (6), 1320–1324.

Henrik, H., Peter, B., 2010. Graphene electrodes for n-type organic field-effect transistors. Microelectron. Eng. 87 (5), 1120–1122.

Jin, Y.H., Jia, M.Q., Zhang, M., Wen, Q.Q., 2013. Preparation of stable aqueous dispersion of graphene nanosheets and their electrochemical capacitive properties. Appl. Surf. Sci. 264, 787–793.

Liu, S., Gu, Y., Wang, S.L., Zhang, Y., Fang, Y.F., Johnson, D.M., et al., 2013a. Degradation of organic pollutants by a Co_3O_4-graphite composite electrode in an electro-Fenton-like system. Chin. Sci. Bull. 58 (19) (2340-234).

Liu, S., Zhao, X.R., Sun, H.Y., Li, R.P., Fang, Y.F., Huang, Y.P., 2013b. The degradation of tetracycline in a photo-electro-Fenton system. Chem. Eng. J. 213, 441–448.

Panizza, M., Cerisola, G., 2009. Electro-Fenton degradation of synthetic dyes. Water Res. 43 (2), 339–344.

Qu, H., Lin, B.Z., He, L.W., Fan, X.R., Zhou, Y., Chen, Y.L., et al., 2013. Electrochemical and photoelectrocatalytic properties of $TaWO_6$ nanosheet film. Electrochim. Acta 87, 724–729.

Raj, M., John, S., 2013. Fabrication of electrochemically reduced graphene oxide films on glassy carbon electrode by self-assembly method and their electrocatalytic application. Phys. Chem. C 117, 4326–4335.

Shinozuka, T., Shirai, M., Tsunooka, M., 2001. Polymers as sulfonic acid generator on irradiation at 146 nm. Eur. Polym. J. 37, 1625–1634.

Shylesh, S., Samuel, P., Srilakshmi, C., Parischa, R., Singh, A.P., 2007. Sulfonic acid functionalized mesoporous silicas and organosilicas: synthesis, characterization and catalytic applications. J. Mol. Catal. A Chem. 274, 153–158.

Wang, H.L., Hao, Q.L., Yang, X.J., Lu, L.D., Wang, X., 2009. Graphene oxide doped polyaniline for supercapacitors. Electrochem. Commun. 11 (6), 1158–1161.

Yan, J., Wei, T., Fan, Z.J., Qian, W.Z., Zhang, M.L., Shen, X.D., et al., 2010. Preparation of graphene nanosheet/carbon nanotube/polyaniline composite as electrode material for supercapacitors. J. Power Sources 195 (9), 3041–3045.

Yuan, W.J., Zhou, Y., Li, Y.R., Li, C., Peng, H.L., Zhang, J., et al., 2013. The edge- and basal-plane-specific electrochemistry of a single-layer graphene sheet. Sci. Rep. 3, 1–6.

Zhang, G.Q., Yang, F.L., Gao, M.M., Fang, X.H., Liu, L.F., 2008. Electro-Fenton degradation of azo dye using polypyrrole/anthraquinonedisulphonate composite film modified graphite cathode in acidic aqueous solutions. Electrochim. Acta 53 (16), 5155–5161.